METHODOLOGY

Open Access

Improvements in the determination of attogram-sized ^{231}Pa in dissolved and particulate fractions of seawater via multi-collector inductively coupled plasma mass spectrometry

Pu Zhang[1,2,3*†], Yanbin Lu[2†], Zhe Zhang[4], Richard Lawrence Edwards[2], Robert Anderson[5,6] and Phoebe Lam[7]

Abstract

A technique is developed to quantify the ultra-trace ^{231}Pa (35–3904 ag) concentration in seawater using multi-collector inductively coupled plasma mass spectrometry (MC-ICP-MS). The method is a modification of the process developed by Shen et al. (Anal Chem 75(5):1075–1079, 2003. https://doi.org/10.1021/ac026247r) and extends it to the application of very low levels of actinides, and the 35 ag ^{231}Pa can be measured with a precision of 15%. The total process blank for the water column was 0.02 ag/g, while the values of the large and small particles were ~ 30 ag/g. The ionization efficiency (ions generated/atom loaded) varies from 0.7 to 2.4%. The measurement time is 2–5 min. The amount of ^{231}Pa needed to produce ^{231}Pa data with an uncertainty of ± 0.8–15% is 35–3904 ag (~ 0.9 × 10^5 to 10 × 10^6 atoms). Replicate measurements of known standards and seawater samples demonstrate that the analytical precision approximates that expected from counting statistics, and that based on detection limits of 52 ag, 55 ag, and 28 ag, protactinium can be detected in a minimum seawater sample size of ~ 2.6 L for small suspended particulate matter (> 0.8 μm and < 51 μm), ~ 3.0 L for large suspended particulate matter (> 51 μm), and ~ 56 mL for filtered (< 0.45 μm) seawater. The concentration of ^{231}Pa (several attograms per liter) can be determined with an uncertainty of ± 2–8% (2σ) for suspended particulate matter filtered from ~ 60 L of seawater. For the dissolved fraction, ~ 1 L of seawater yields ^{231}Pa measurements with a precision of 0.8–10%. The sample size requirements are several orders of magnitude less than traditional decay-counting techniques, and the precision is better than that previously reported for ICP-MS techniques. Our technique can also be applied to other environmental samples, including river, lake, and cave water samples.

Keywords ^{231}Pa, MC-ICP-MS, Suspended particulate matter, Precision, Reproducibility

†Pu Zhang and Yanbin Lu have contributed equally to this work and share first authorship.

*Correspondence:
Pu Zhang
zhangpu035@cdut.edu.cn
Full list of author information is available at the end of the article

Springer Open

Zhang *et al. Progress in Earth and Planetary Science*   (2023) 10:65

Page 2 of 11

1 Introduction

^{231}Pa is the only long-lived intermediate daughter product of ^{235}U ($t_{1/2} = 32{,}760$ years) (Robert et al. 1969) and has been broadly applied as a geochemical tracer in fields as diverse as oceanography, geochronology, and paleoclimatology (Anderson et al. 1983; Asmerom et al. 2000; Bradtmiller et al. 2014; Edmonds et al. 1998; Edwards et al. 1997; Hayes et al. 2014, 2015; Hoffmann et al. 2013; Moran et al. 1997). It is noteworthy that the concentrations of ^{231}Pa and ^{230}Th in seawater and sediments, as well as their isotopic ratios, can elucidate the representative processes responsible for the removal of particle-reactive elements from the ocean (Anderson et al. 1983; Chase et al. 2003; Hayes et al. 2015; Kretschmer et al. 2011; Lao et al. 1993; Luo and Ku 1999, 2004; Siddall et al. 2005; Walter et al. 1997, 2001). The ^{231}Pa and ^{230}Th in seawater not only contribute to the clarification of the mechanisms of global ocean circulation processes but also deepen our understanding of the paleoenvironmental record, including processes such as boundary scavenging (Anderson et al. 1983; Hayes et al. 2014, 2015; Kretschmer et al. 2011; Moran et al. 2001, 2002) and ventilation of the modern (Deng et al. 2014; Edmonds et al. 1998; Thomas et al. 2006) and last-glacial (Bradtmiller et al. 2014; Thomas et al. 2007) periods in the Atlantic, Pacific, Indian, and Arctic oceans.

^{231}Pa has an extremely low natural abundance in the marine environment, leading to uncertainty in its measurement. In surface seawater, the dissolved fraction of ^{231}Pa is ~ 500 ag/L, while the particulate fraction is only 10 ag/L (Deng et al. 2014; Edmonds et al. 1998; Hayes et al. 2014; Moran et al. 2001, 2002; Thomas et al. 2006). There are differences in the precisions and the required sample sizes of the different techniques. For example, the traditional α and ß counting techniques typically yield a precision of ± 9–28% (2σ) for the determination of ^{231}Pa (100–4000 fg) (Anderson and Fleer 1982). In addition, these methods require larger sample sizes (~ 75 large samples per measurement batch) and longer counting times (Anderson and Fleer 1982; Anderson et al. 1983; Nozaki and Nakanishi 1985). Thermal ionization mass spectrometry (TIMS) was first applied by Pickett et al. (1994) to perform Pa measurements with a precision of better than ± 1% for sample sizes of hundreds of femtograms of ^{231}Pa. Subsequently, Shen et al. (2003) used TIMS with a precision of ± 4–12% (2σ) for samples containing 100–1000 ag ^{231}Pa ($\sim 3 \times 10^5$ to 3×10^6 atoms). TIMS has been widely used for the determination of ^{231}Pa in different natural materials, such as carbonates, silicates, and seawater (Edmonds et al. 1998; Edwards et al. 1997; Pickett and Murrell 1997). In addition, inductively coupled plasma mass spectrometry (ICP-MS) has also been used for the measurement of ^{231}Pa in both dissolved and particulate forms throughout ocean water profiles. This method improves the detection limits and sample size requirements and has a precision of $\sim \pm 2$% for 100–200 fg seawater samples (Choi et al. 2001). In contrast to the above techniques, a multi-collector inductively coupled plasma mass spectrometry (MC-ICP-MS) technique with lower detection limits and a higher precision is proposed in this study. This technique can be applied to various special environments, for example, the detection of small (0.8–51 μm) and large (> 51 μm) particles and surface dissolved samples with low ^{231}Pa concentrations in the Arctic with a better precision. The division of the particle size is of great oceanographic importance (Hayes et al. 2015). It has also been shown that scavenging intensity for the natural radionuclides ^{230}Th and ^{231}Pa can vary with particle type in ocean. Changing proportions of particle types over geologic time may overprint other influences on the sediment record. While previous work has shown that there is still debate about what are the major carrier phases. The research result of Hayes et al. (2015) suggests that a negligible fraction of Pa or Th exists in the 0.45–0.8 μm size class. Most of Pa and Th exist in particle of size 0.8–51 μm size. The particle collected in ocean includes lithogenic material, particulate organic matter, calcium carbonate, biogenic opal and authigenic Fe and Mn oxides. And absorbed ^{230}Th is mainly originating from decay of ^{234}U in dissolved seawater namely < 0.45 μm. Absorbed ^{230}Th originating from dissolution of U-bearing minerals usually exists small particulate about 0.8–51 μm. Particulate ^{230}Th originating from decay of ^{234}U within intact mineral lattices usually exists large particulate (> 51 μm). This detailed classification of particle size is fully linked to the differences in the chemical behavior of the ^{231}Pa and ^{230}Th being measured.

(1) Samples passing through 0.8 μm filters contain colloidal U and dissolved U, and a negligible fraction of Pa or Th exists in the 0.45–0.8 μm size class. In the water column, Th has a tetravalent oxidation state with a high particle adsorption that is consistent with Pa, and the Pa in the water column is readily absorbed onto suspended particulate matter. (2) Samples between the 0.8 μm and 51 μm filters contain small particles, which usually occur in the convergence, adsorption, and reconvergence processes in the water column due to the slow settling velocity. (3) Samples passing through 51 μm filters usually exist as large particle and usually have a fast settling velocity, indicating that the detrital component in the water column is less affected before sinking to sediments and the sizes of the particles have with oceanographic significance. Among them, the Arctic surface dissolved fraction contains ~ 70 ag/L, and the ice hole contains ~ 30 ag/L. In addition, there are differences in the particulate

fraction of ^{231}Pa at different depths in the same environment (Additional file 1: Figs. S1 and S2). The small particulate fraction of ^{231}Pa in the Pacific surface seawater is only 3 ag/L (10^{-21}–10^{-20} molar or 10^3–10^4 atoms/L), while the large particulate fraction at a depth of ~1000 m is 15 ag/L. The particulates analyzed are mainly inorganic particles with a limited organic effect. The concentrations of the elements in the dissolved fraction cannot be measured via ICP-MS due to the high detection limits of several ppb and ppt. All of the samples measured in this study were at the ag and fg levels. The ^{230}Th and ^{231}Pa concentrations of the particulates with sub-fg and sub-pg concentrations also cannot be measured via ICP-MS or CHNS analysis because of the high detection limits of several ppb and ppt. All measured samples here are all ag and fg levels. ^{230}Th and ^{231}Pa of particulate with sub-fg and sub-pg also cannot be measured by ICP-MS or CHNS analysis because of high detection limits getting to ppb and ppt. In conclusion, the quantification of ultra-trace ^{231}Pa (35–3904 ag) concentrations in seawater via MC-ICP-MS is available for the measurement of samples of several orders of magnitude at the ag and fg levels, and this extension of the determination of very low ^{231}Pa concentrations is both novel and challenging.

The lowest value previously reported for the blanks was 16 ± 15 ag (Shen et al. 2003), and the detection limits were 38 ag for particulate matter and 49 ag for the dissolved fraction. In this study, we mainly modified the method proposed by Shen et al. (2003), and the main contribution of this study is the characterization and testing of this method for very small protactinium loads in the dissolved fractions of seawater for small and large particulates (Fig. 1). The signal/noise ratio was improved due to the high ionization efficiency and fast analysis of a large-quantity samples with a limited analysis time in a case producing more ^{233}U decayed from ^{233}Pa (decay constant $\lambda_{223Pa} = 0.0256486$ d^{-1}) for analysis with a slow time. However, the application of MC-ICP-MS to the analysis of the seawater particulate and dissolved fractions containing as little as tens of attograms of Pa still remains challenges. (1) The procedural blank should be kept at as a low level as possible. (2) A high ionization efficiency must be maintained (e.g., ~0.7–2.4%). (3) Measurements with small ion beams must be precise and accurate. Among the other characteristics, a low detector dark noise is required. With the introduction of ^{233}Pa ($t_{1/2} = 27.0$ days; Jones et al. 1986) as a spike in MC-ICP-MS analysis, the dark noise inevitably increases. Due to the decay of ^{233}Pa to ^{233}U in a short time range, the dark noise of the detector increases from 70 to 143 cpm in 10 h. When the samples have been measured, we increase the machine sensitivity (ionization efficiency get to from 0.7 to 2.4%) to obtain a high signal/noise ratio when we measure sample in a limited time from 2 to 5 min/per sample. TIMS analysis of ^{233}Pa is slow, usually ~1 h/per sample, which is not good for a large quantity of samples per batch, because of the short decay time from ^{233}Pa to ^{233}U in the entire analysis period. 4) A high sample throughput is required to obtain large-scale ocean ^{231}Pa data. The analysis of ultra-trace ^{231}Pa in the dissolved seawater and particulate fractions requires the method with small sample sizes, short measurement times, a low procedural blank, a high instrumental sensitivity, and a high signal/noise ratio. In this study, we mainly utilized MC-ICP-MS to determine the concentration of ultra-trace ^{231}Pa (35–3904 ag) in seawater. This method is feasible and has a better sample size, precision, and accuracy than previously reported ICP-MS techniques.
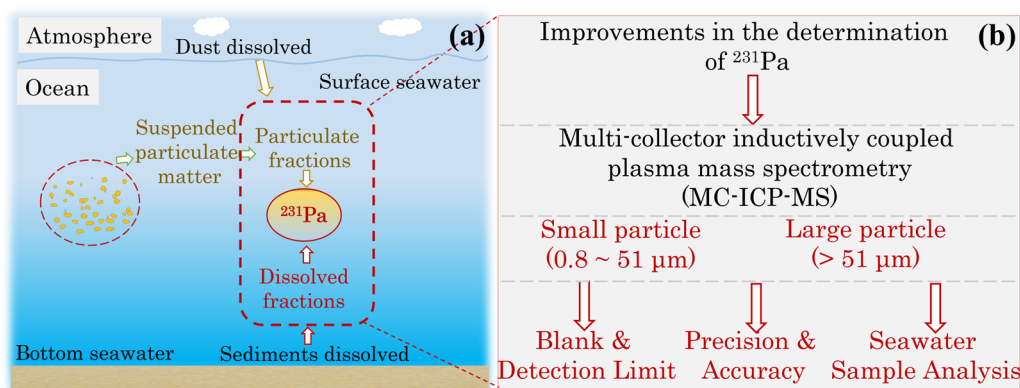
Fig. 1 **a** Natural processes of ^{231}Pa in seawater and **b** procedures for the determination of ^{231}Pa concentration via the modified MC-ICP-MS technique developed in this study

2 Experimental methods

2.1 Reagents and materials

This study was performed in the clean room at the Minnesota Isotope Laboratory (MIL) for chemical procedure analysis. A Super-Q purification system was used to purify the deionized/distilled water, and the bottles and beakers were cleaned in an acid vat (Edwards 1988). The ultrapure reagents were obtained from Aristar Ultra Chemicals, including HCl, HF, $HClO_4$, and NH_4OH. The redistilled HNO_3 was obtained from GFS Chemicals Inc. First, 200 g of anion-exchange resin (Spectrum Spectra Gel, AG 1-X8, 100–200 mesh) was filled into a quartz column and was sequentially cleaned using the following cleaning steps: (1) 250 mL of H_2O, 250 mL of 14 M HNO_3; (2) 500 mL of H_2O; (3) 250 mL of H_2O, 250 mL of 14 M HCl; (4) 500 mL of H_2O; (5) 490 mL of H_2O, 10 mL of HCl; and (6) 500 mL of H_2O. The columns used for the ion separation were constructed of heat-shrink Teflon tubing (4:1, ½ in.) from Texloc Ltd. and were cleaned sequentially via boiling in aqua regia, AR HNO_3 (7 M), AR HCl (5 M), distilled HNO_3 (0.1 M), and Aristar Ultra HCl (0.1 M).

2.2 ^{223}Pa spike solution preparation

Our modification of the ^{237}Np milking method described by Shen et al. (2003) was to obtain the internal standard (^{233}Pa), which is described below. The measurement conditions and improved separation methods for MC-ICP-MS are presented in Additional file 1 (Tables S1 and S2).

(1) The solution in the stored Np vial was dried, and five drops of $HClO_4$ were added to the ^{237}Np solution. (2) The solution was dried, redissolved using 1 column volume (cv) of 9 M HCl, and passed through an 850 μL ion-exchange column, and the eluant was collected in the Np vial. (3) The Pa fraction was eluted twice via the addition of 2 CVs of 9 M HCl + 0.05 M HF to the Pa vial. The collected Pa solution was dried using three drops of $HClO_4$. (4) The Np fraction was eluted into the Np vial by adding 8 CVs of 1 M HCl + 0.5 M HF. (5) The collected Pa fraction was dissolved using 1 cv of 9 M HCl + 0.05 M HF and was loaded into column 2. (6) Steps (3), (4), and (5) were repeated 10 times in columns 2 and 3 to purify the Pa from the Np. (7) The collected Pa fraction was dissolved using 1 cv of 9 M HCl and was loaded into column 4. The Th fraction was eluted twice via the addition of 2 CVs of 9 M HCl to the Np vial. (8) The Pa fraction was eluted twice via the addition of 2 CVs of 9 M HCl + 0.05 M HF to the Pa vial. The collected Pa solution was dried using three drops of $HClO_4$. (9) Steps (7) and (8) were conducted one time in column 5 to further purify the Pa from Th interference. After collecting the last Pa fraction, the solution was dried and redissolved using five drops of HNO_3. In a clean room, the Pa solution was diluted to ~ 100 mL using 1 M HNO_3 + 0.05 M HF and at heated at 70 °C overnight to equilibrate the spike solution.

2.3 Standards and samples

The ^{231}Pa solutions (Pa-I, 3.04×10^9 atoms/g; Pa-II, 4.09×10^9 atoms/g) were separated from the uranium ore solutions. The ^{231}Pa was calibrated using a ^{233}Pa tracer solution, which was calibrated with a ^{233}Pa tracer solution, which was calibrated with a solution of a zircon from the Piper Gulch Granodiorite that records concordant U-Pa ages (Asmerom et al. 1990) and may be in secular equilibrium with ^{234}U and ^{230}Th (Cheng et al. 2000). Interlaboratory calibration between the Minnesota Isotope Lab (based on the same mixed ^{231}Pa–^{230}Th–^{232}Th) and Lamont Laboratory demonstrated that the independent calibrations were reproducible to better that 0.2% (Edwards et al. 1997). A more dilute standard (Pa-III, 1.85×10^9 atoms/g or 710 fg/g) was prepared via dilution of an aliquot of Pa-I.

The particulate fraction of seawater samples (~ 500 L) collected from three depths (25–5000 m) in the Pacific was used for the replicate analyses. An additional 25 seawater samples (including dissolved samples collected in the Arctic during Geotrace 2015 and small and large particulate fractions collected in the Pacific during Geotrace 2013) were filtered through an acid-cleaned 51 μm pore-size Sefar polyester mesh prefilter and a 0.8 μm pore-size Pall Supor 800 polyethersulfone filter, and approximately 500 L of seawater was filtered to collect the particulate fractions. The filtered seawater samples were stored and acidified (20 mL of 6 M HCl) in acid-cleaned polyethylene bottles.

2.4 Chemical analysis

The chemical procedures were optimized according to the methods used in previous studies, and Th samples were also collected. The measurement time has been 2–5 min according to the sample content based on the signal/noise ratio, usually the signal of ^{233}Pa is 600 cps. When we measured a 1 L sample, the ^{231}Pa content of the sample varied from 35 to 4000 ag. The dissolved fractions of the seawater samples were acidified (pH of ~ 2) using 6 M HCl, 30–80 fg of ^{233}Pa tracer was added, and 450 mg of Fe was added to 1 L of dissolved sample. To ensure sample-spike equilibrium, the solution was shaken by hands for 4 days, and then, NH_4OH was added to the solution to co-precipitate Pa with Fe $(OH)_3$ (pH of 8–9 for this solution). The concentration of ^{231}Pa (35–3904 ag) in seawater is an ultra-trace level, and the background value of ^{231}Pa is very low. A large number of samples (~ 56) were analyzed in the first batch and the other 28 samples were analyzed in the second batch to avoid contamination,

Zhang *et al. Progress in Earth and Planetary Science*   (2023) 10:65

Page 5 of 11

and more magnetic stirrers were used at the same time. We preferred the hand-shaking method to the magnetic stirrer method. Hand shaking was conducted for 2 days during the experimental phase. Each sample was shaken hourly and eight times per day to ensure adequate mixing of the solution, diluent, and $FeCl_2$. The sample was then left to stand for 2 days in order to achieve effective flocculation and precipitation of $Fe(OH)_3$ using $NH_3 \cdot H_2O$. The overall chemical procedure yield was determined by measuring the [233]Pa content of the diluent, and the yield consistently exceeded 90%. The replicate sample results of every batch were accurate within the error, and the results of the surface water (SW) standards STD 2010-1 and STD 2015-1 for every batch with the same column chemistry were also consistent within error. This precipitate was allowed to settle for 1–2 days before the overlaying seawater was siphoned off. Then, the Fe precipitate was transferred to a centrifuge tube for centrifugation and as rinsed with deionized H_2O (>18 MΩ) to remove the major ions from the seawater. The precipitate was then dissolved in 14 M HNO_3 and transferred to a Teflon beaker. It was then dried and subjected to anion-exchange chromatography in 7 M HNO_3 using AG1-X8, 100–200 mesh-size resin, and a polyethylene frit. The initial separation was performed in Teflon columns with a 0.75 mL column volume. The sample was loaded in one CV of 7 M HNO_3, followed by the addition of 1.5 CVs of 7 M HNO_3, 3 CVs of 8 M HCl (to collect the Th fraction), and 3 CVs of 8 M HCl+0.015 M HF (collect Pa fraction). The Pa and Th fractions were then dried down in the presence of two drops of $HClO_4$ and dissolved in 7 M HNO_3. They were each passed through the second and third columns (each with a 0.5 mL column volume) using similar elution schemes. The final Pa and Th fractions were then dried down in the presence of two drops of $HClO_4$ and were dissolved in 2% HNO_3+0.01% HF for analysis on the mass spectrometer.

The filtered particulate fraction was analyzed as follows: 1/8 of a filter was placed in a 30 mL Teflon beaker, and the aliquots of the artificial isotope yield monitors of [229]Th and [233]Pa were weighed. The filters were completely submerged in 7 M HNO_3 combined with 10 drops of HF, were tightly capped with a Teflon threaded cap, and were heated for 10 h at ~93.3 °C (200°F) to dissolve/leach the particulate samples under pressure. The leached solution was then transferred to a second acid-cleaned Teflon beaker and was separated from the remaining filter, and then, five drops of $HClO_4$ were added to the leached solution in the second beaker. The original beaker walls and caps were washed with small amounts of diluted HNO_3 for low concentration ~10% and the resulting solution was added to the second beaker. The solution was then dried down, dissolved in

2 M HCl, and transferred to a 15 mL centrifuge tube, along with the 2 M HCl rinse solution. One drop of dissolved Fe and six to nine drops of NH_4OH were added to raise the pH to 8–8.5, at which time the iron (oxy) hydroxide precipitated. This precipitate was then centrifuged, decanted, washed with deionized H_2O (>18 MΩ), centrifuged, dissolved in 14 M HNO_3, and transferred to a Teflon beaker. It was then dried down and dissolved in 7 M HNO_3 for anion-exchange chromatography using AG1-X8, 100–200 mesh resin, and a polyethylene frit. The initial separation was performed using Teflon columns (internal diameter of ~0.35 cm) with a ~0.55 mL column volume. The sample was loaded in one CV of 7 M HNO_3, followed by 1.5 CVs of 7 M HNO_3, 3 CVs of 8 M HCl (collection of Th fraction), and 3 CVs of 8 M HCl+0.015 M HF (collection of Pa fraction). The Pa and Th fractions were then dried down in the presence of two drops of $HClO_4$ and were dissolved in 7 M HNO_3. They were each passed through the second and third columns (each with a column volume of ~0.55 mL) using similar elution schemes. The final Pa and Th fractions were then dried down in the presence of two drops of $HClO_4$ and were dissolved in 2% HNO_3+0.01% HF for mass spectrometer analysis. The chemical recoveries were typically 90–95% for the dissolved and particulate fractions.

The concentrations of [232]Th, [230]Th, and [231]Pa were calculated via isotope dilution using nuclide ratios determined on a Thermo-Finnigan Neptune mass spectrometer. All of the measurements were conducted using a peak jumping routine in ion counting mode on the discrete dynode multiplier after the retarding potential quadrupole. A total of 50–250 sets of data were measured for each sample. Since the centering of peaks could not be easily verified with small ion beams for [231]Pa and [233]Pa, an additional mixed [231]Pa–[233]Pa standard was used for this purpose. A solution of [233]U–[236]U tracer was analyzed to determine the mass deviation correction (assuming that the mass fractionation for Th and Pa was the same as that for U). Each sample measurement was bracketed by measurements of an aliquot of the run solution in order to correct for the influence of the instrument background count rates on the masses measured. The analyses (MC-ICP-MS) were conducted within 24 h of the chemical processing, and the study revealed that the small amount of [233]U produced via the decay of [233]Pa during this interval evaporated prior to the start of the data acquisition to diminish this isobaric interference, i.e., to minimize the decay of [233]Pa to [233]U in the Pa cut (Thomas et al. 2006). Throughout the analysis, the multiplier dark noise gradually increased from an initial value of <1.0 counts per second (cps) to 1.2–1.4 cps due to the introduction of the short-lived [233]Pa radionuclide. This

Zhang *et al. Progress in Earth and Planetary Science*   (2023) 10:65

Page 6 of 11

background dark noise was tracked between samples, and a correction was applied during the data processing.

An aliquot of two intercalibrated working standard solutions of ^{232}Th, ^{230}Th, and ^{231}Pa, SW STD 2010-1 and STD 2015-1, were added to a separate acid-cleaned Teflon beaker along with weighed aliquots of the ^{229}Th spike and ^{233}Pa spike. The spike and standard were equilibrated for 3 days. They were then dried down and dissolved in 7 M HNO$_3$ for anion-exchange chromatography using AG1-X8, 100–200 mesh-size resin, and a polyethylene frit, and they were also processed using the sample procedure used for the samples. The procedural blanks for the chemical and mass spectrometric analyses conducted in the Minnesota lab were approximately 28 ag for ^{230}Th and 18 ag for ^{231}Pa.

An improved and more consistent ionization efficiency of 0.7–2.4% was used for the sample measurement, which was better than our previous work (ionization efficiency of 3–5‰) (Shen et al. 2003). Additional advantages include a reduced measurement time, from ~1 h to 2–5 min, and an increased ion beam intensity. The typical beam intensities for ^{231}Pa and ^{233}Pa were 8–470 cps and 800–5000 cps, respectively, and thus, the signal/dark noise ratio was increased by a factor of 3–6.

2.5 Data processing

We completed the data processing offline, and the measurements were calibrated sequentially, including mass fractionation correction, instrumental tail correction, diluent factor adjustment, blank subtraction, and internal growth correction for ^{231}Pa and ^{230}Th. The uncertainties were calculated to be at the 2σ level, representing the maximum of the counting statistics. The corrections were fully propagated via mass fraction correction, dark noise, abundant sensitivity, blanks, and spikes. The abundance sensitivity was 2.6×10^{-7} at a one atomic mass unit (amu) difference and 5.2×10^{-8} at a 2 amu difference after the RPQ filter. Radioactive decay corrections were performed for the ^{233}Pa in the spike solution between calibration and analysis time.

3 Results and discussion

3.1 Blank and limit of detection

After 11 separation and purification step repetitions of the ^{233}Pa spike from the ^{237}Np solution, the ^{231}Pa was no longer measurable (^{231}Pa/^{233}Pa < 7 ppm) and the amount of ^{231}Pa in each sample was negligible. The total ^{231}Pa blank from the chemicals (including the spikes, resins, iron, and acids) in the dissolved sample was 0.02 ± 0.006 ag/g (Table 1). The total procedural blanks, including filtration, were 34 ± 6 ag/g (1/8 filter) (0.8 µm Pall Supor800 polyethersulfone filters) and 29 ± 8 ag/g (1/8 filter) (51 µm

Sefar polyester mesh prefilter), all of which are used for the seawater particulate sampling (Table 1).

The dark noise in our system was ~1.0 cps, and the noise/signal ratio was typically between 5 and 10% for samples with ^{231}Pa < 0.3 ag/g, and less than 3% for the samples had ^{231}Pa > 0.4 ag/g (Fig. 2). On the basis of the general definition of the detection limit, the blank + 3δ_B, where δ_B is the standard deviation of the blank, the minimum detectable amount of the dissolved sample ^{231}Pa was 38 ag, that for using one-eighth of a 0.8 µm Pall Supor800 polyethersulfone filter was 52 ag, and that for using one-eighth of a 51 µm Sefar polyester mesh prefilter was 53 ag.

3.2 Precision and accuracy

The precision is eventually constrained by the counting statistics: $2\sigma = 2\,(N^{-1/2})$, where N is the total number of ions counted. Due to the high ionization efficiency (0.7–2.4%), the high ^{231}Pa ion beam to dark noise ratio (9–457), and the low procedural blank (0.02 ag/g), the ^{231}Pa measurements had a precision of 1–3.9 ag/g (0.8–2%), including the counting error for ^{233}Pa. Figure 2 shows the relationship between the sources of error (including the sample size, chemical blank, and mass fractionation correction) and the total analytical uncertainty for the Pacific seawater particulate samples and Arctic seawater dissolved samples. For samples containing ^{231}Pa > 0.3 ag/g, the Pa counting error accounted for the majority of the total uncertainty, and the procedural blank accounted for less than 7%. For samples containing ^{231}Pa < 0.3 ag/g, the intensity of the ^{231}Pa ion beam was always less than 8 cps. When the amount of ^{231}Pa was less than 0.1 ag/g, the portion of the total uncertainty caused by the counting error was less than 10%, and the portion caused by the blanks was greater than 20%.

The results from replicate analyses of the ^{231}Pa-2010 and ^{231}Pa-2015 standards are presented in Table 2. The internal precision (intra-run) was 0.5% for a sample size of 18 fg. For multiple measurements of the sample sizes, the external uncertainties (between-runs) were comparable to the internal uncertainties for small particulates. These results indicate that the internal uncertainty was an accurate measure of the true uncertainty. The key sources of this uncertainty were the counting statistics (primarily for samples greater than 300 ag) and the blank correction uncertainties (primarily for samples less than 100 ag). The measured concentrations for all of the replicates were consistent with the gravimetric measurements and with measurements obtained in the Lamont–Doherty Earth Observatory (LDEO) Laboratory, Columbia University (Table 2), indicating that the MC-ICP-MS technique is accurate overall.

Zhang *et al. Progress in Earth and Planetary Science*　(2023) 10:65

Page 7 of 11

Table 1 The total amount of [231]Pa in the blank derived from the chemicals, including the spike, resin, Fe, and acids, and the total procedural blank, including filtering for an acid-cleaned 0.8 μm Pall Supor800 polyethersulfone filter (for small particulates) and 51 μm Sefar polyester mesh prefilter (for large particulates)

Sample no.	[231]Pa (ag/g)	Error /(2σ)	Sample type
Chem-blank-1	0.015	0.008	Dissolved
Chem-blank-2	0.013	0.006	Dissolved
Chem-blank-3	0.025	0.008	Dissolved
Chem-blank-4	0.020	0.003	Dissolved
Chem-blank-5	0.025	0.004	Dissolved
Average	0.020	0.006	
Sample no.	**[231]Pa (ag/g(1/8filter))**	**Error /(2σ)**	**Sample type**
GT8735db	65.559	0.011	Small particulate
GT8702db	8.212	0.003	Small particulate
GT9004db	25.652	0.007	Small particulate
GT9062db	29.761	0.006	Small particulate
GT9587db	50.132	0.006	Small particulate
GT9594db	34.950	0.005	Small particulate
GT9966db	85.845	0.012	Small particulate
GT9971db	38.720	0.006	Small particulate
GT8292db	11.115	0.001	Small particulate
GT8348db	62.386	0.004	Small particulate
GT3160db	16.289	0.008	Small particulate
GT3193db	9.858	0.004	Small particulate
GT2441db	16.165	0.004	Small particulate
GT2326db	9.326	0.006	Small particulate
GT2276db	41.427	0.009	Small particulate
Average	33.693	0.006	
GT8824dbQP	21.450	0.009	Large particulate
GT8735dbQP	60.654	0.011	Large particulate
GT8702dbQP	26.372	0.008	Large particulate
GT9253dbQP	22.628	0.006	Large particulate
GT9971dbQP	27.383	0.009	Large particulate
GT3160dbQP	17.800	0.006	Large particulate
Average	29.381	0.008	

3.3 Seawater sample analysis

The ionization efficiency was 1.0% when [231]Pa was analyzed via MC–ICP-MS, and the precision was ± 0.8–6% when the sample size was 100–3900 ag [231]Pa. As a result, we would need 5 L of surface seawater ([231]Pa of ~ 20 ag/L) or 2 L of deep seawater ([231]Pa of ~ 50 ag/L) in order to obtain suspended particulate matter samples of this precision via filtration (Moran et al. 2001, 2002). In contrast, 0.2 L of seawater ([231]Pa of 500–4000 ag/L) was required for the dissolved fraction samples (Moran et al. 2001, 2002). With respect to the detection limits, the minimum surface seawater sample size was 2.5 L for the particulate fraction and 0.2 L for the dissolved fraction. Therefore,

for routine seawater [231]Pa analyses, we recommend sample sizes of 0.5–1 L for the dissolved fraction and 5–10 L for the suspended particulate fraction.

Figure 3 presents the results of the replicate analyses of seawater (Arctic and Pacific) and small/large particulate samples (Pacific). The dissolved and small particulate samples are consistent with each sampling depth within the margin of error. The similarity of the magnitudes of the external and internal uncertainties for each sample shows that the internal error can represent the true precision. Nevertheless, the external uncertainties for the Pacific large particle samples are larger than the individual internal uncertainties (Fig. 3c), indicating that
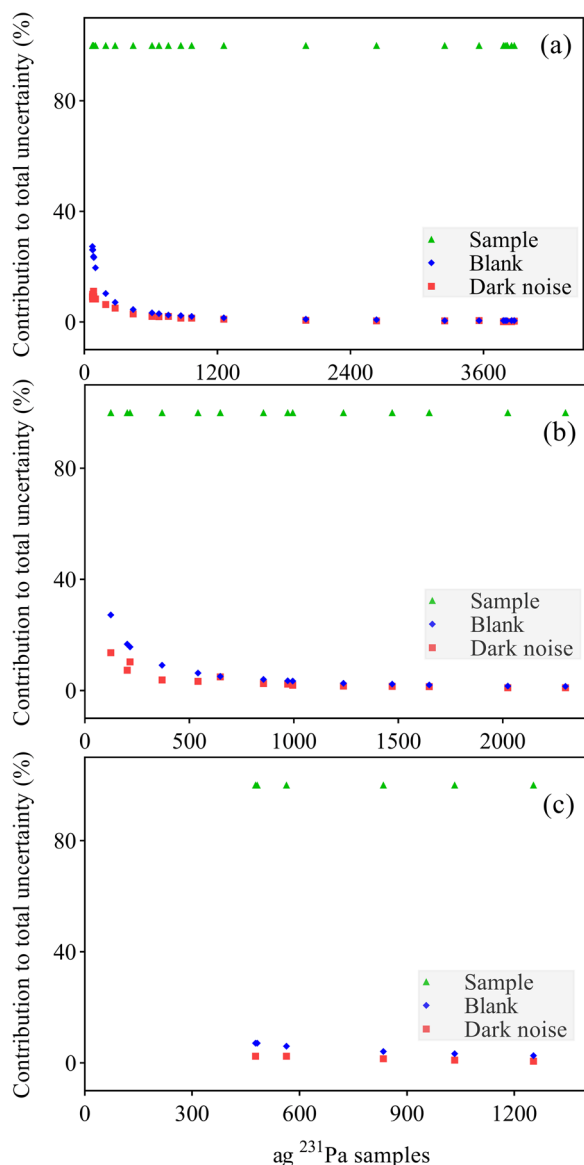
Fig. 2 Relationship between the analytical uncertainty for the sample (triangle), chemical blank (diamond), and secondary electron multiplier (SEM) dark noise (squares) and the amount of ^{231}Pa measured in **a** the dissolved fraction of 25 seawater samples, **b** the small particulate fraction of 14 seawater samples, and **c** the large particulate fraction of six seawater samples. The seawater dissolved samples were collected from the Pacific Ocean and the particulate samples were collected from the Arctic Ocean

Table 2 Replicate analyses of the ^{231}Pa-2010 and ^{231}Pa-2015 standards

Sample no.	^{231}Pa ($\times 10^3$ ag/g)	Error (2σ)	Notes	Measured in Lab
LDEO 2015-1	39.00	1.36	STD 2015-1	LDEO
LDEO 2010-1	37.50	1.87	STD 2010-1	LDEO
STD 2010-1	37.78	0.29	STD 2010-1	UMN
STD 2010-2	37.63	0.20	STD 2010-1	UMN
STD 2010-3	37.63	0.18	STD 2010-1	UMN
STD 2010-4	37.92	0.18	STD 2010-1	UMN
STD 2010-1-ave	37.74	0.21		
STD 2015-1	39.58	0.16	STD 2015-1	UMN
STD 2015-2	39.20	0.15	STD 2015-1	UMN
STD 2015-3	38.79	0.32	STD 2015-1	UMN
STD 2015-4	39.42	0.22	STD 2015-1	UMN
STD 2015-5	38.73	0.16	STD 2015-1	UMN
STD 2015-6	39.23	0.17	STD 2015-1	UMN
STD 2015-7	39.25	0.17	STD 2015-1	UMN
STD 2015-1-ave	39.17	0.19		

LDEO Lamont-Doherty Earth Observatory, Columbia University, *UMN* University of Minnesota

the internal errors may not be representative of the true precision of the large particulate samples, but the external uncertainty was predominantly less than 12%. The suspended particulate matter samples obtained filtering ~500 L seawater at different depths through 1/8 of a filter contained 200–2000 ag of ^{231}Pa and had a measurement accuracy of ±1.0–5.6%. The precision of the two replicates of one particle sample was ±1.5–5.9% from two replicates of six small particulate samples obtained via 1/8 filtration of ~500 L of seawater containing 200, 280, 380, 1830, and 5780 ag. All of the samples were from the Geotrace program. The particulate matter is not only for Pa and Th but also for the analysis of other trace metal elements (Schlitzer et al. 2018), and all of the samples were filtered in the field when sampling seawater. The concentration detection limit was also useful for particles. Due to the heterogeneity of the particulate matter, in this study, 1/8 of a filter was used uniformly for the chemical analysis, and realistic sample sizes were used to obtain reproducible evaluation results. This method is useful for sub-femtogram size applications, with an error of ~1%, and it is useful for attogram size applications, with an error of ~15% (Fig. 3). From two replicates of five large particulate samples, two replicates of one large particulate sample were analyzed with an accuracy of ±1–20% for 1/8 filtration of ~500 L of seawater from depths of 900–3900 m, with a ^{231}Pa content of 500–3800 ag. The results demonstrate that the ^{231}Pa chemically separated from the seawater had essentially the same analytical power as the ^{231}Pa in the standard solution.

4 Conclusions

In this study, we improved and characterized the MC-ICP-MS technique for measuring attogram-sized ^{231}Pa concentrations in filtered seawater and particulate
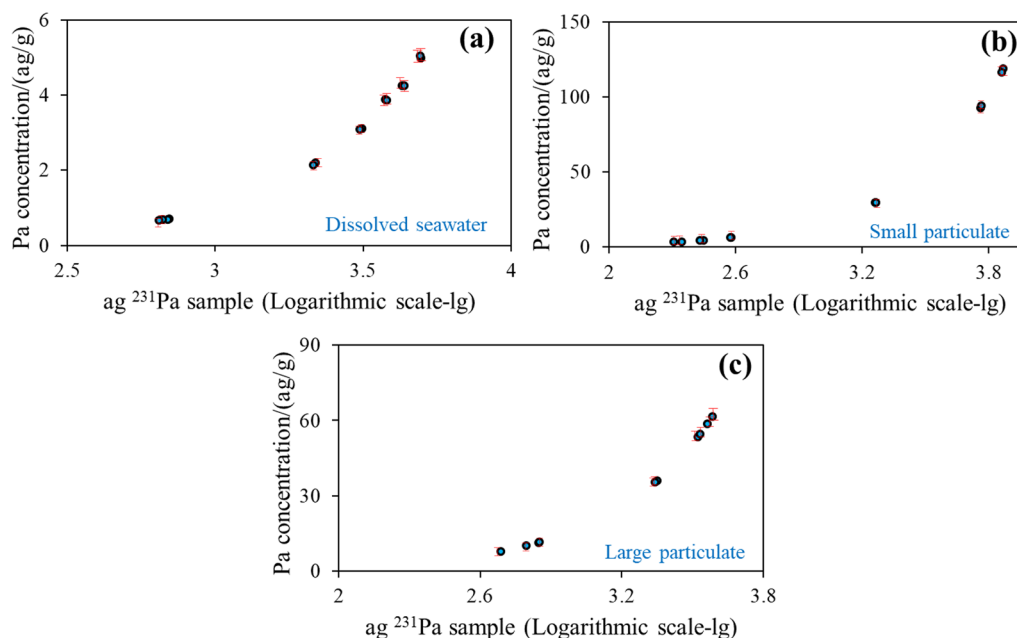
Fig. 3 Replicate measurements of the dissolved seawater sample from the Arctic and the two particulate fractions filtered from the seawater collected from the Pacific: **a** concentration of ^{231}Pa per gram of dissolved seawater; **b** concentration of ^{231}Pa in the small particles (0.8–51 μm); **c** concentration of ^{231}Pa in the large particulate matter (> 51 μm). The blue color in the three panels indicates the actual measured concentration of ^{231}Pa in the sample, and the red color indicates the corresponding measurement error or uncertainty

matter samples. Compared to previous ICP-MS methods, the chemical blanks had low levels in our study. The total process blank for the water column was 0.02 ag/g, while the concentrations of the large and small particles were ~ 30 ag/g. Considering the higher ionization efficiency of the samples (0.7–2.4%), we achieved a relatively high ion beam signal to dark noise ratio, resulting in the results having reduced sample size capabilities (< 100 ag ^{231}Pa). In addition, a large volume of water sample is often required for routine seawater ^{231}Pa analyses, but in this study, we achieved a reduction in the sample volume. We recommend volumes of 0.5–1 L for the dissolved phase and 5–10 L for the suspended particulate matter. In addition, for the fluctuation of the dark noise during the sample analysis, we evaluated the stability of the dark noise via multiple corrections of the dark noise, multiple mass fractionation of ^{236}U/^{233}U (U-F), and cross-assessment of Pa standards STD 2010-1 and STD 2015-1. In summary, measuring ultra-trace ^{231}Pa (35–3904 ag) concentrations in seawater using MC-ICP-MS is applicable to measurement of samples with ag to fg concentrations. This method is not only applicable to surface water and deep water but also has broad applications to other earth science fields, including ^{235}U–^{231}Pa geochronology, igneous geochemistry, and paleoclimatology.

Supplementary Information

The online version contains supplementary material available at https://doi.org/10.1186/s40645-023-00600-z.

Additional file 1. Supplementary information include ^{231}Pa measurements method has been used in natural sample analysis of Pacific and Arctic; Measurement conditions of MC-ICP-MS; A flowchart of the new and improved ^{233}Pa separation and purification method.

Zhang *et al. Progress in Earth and Planetary Science*   (2023) 10:65

Page 10 of 11

Declarations

Competing interests
The authors declare that they have no competing interests.

Author details
[1]College of Earth Sciences, Chengdu University of Technology, Chengdu, China. [2]Department of Earth and Environmental Sciences, University of Minnesota, Minneapolis, MN, USA. [3]College of Urban and Environmental Sciences, Northwest University, Xi'an, China. [4]College of Environmental Science and Engineering, Nankai University, Tianjin, China. [5]Lamont-Doherty Earth Observatory of Columbia University, Palisades, NY, USA. [6]Department of Earth and Environmental Sciences, Columbia University, New York, NY, USA. [7]Department of Ocean Sciences, University of California, Santa Cruz, CA 95064, USA.

References

Anderson RF, Fleer AP (1982) Determination of natural actinides and plutonium in marine particulate material. Anal Chem 54(7):1142–1147. https://doi.org/10.1021/ac00244a030

Anderson RF, Bacon MP, Brewer PG (1983) Removal of ^{230}Th and ^{231}Pa from the open ocean. Earth Planet Sci Lett 62(1):7–23. https://doi.org/10.1016/0012-821x(83)90067-5

Asmerom Y, Zartman RE, Damon PE, Shafiqullah M (1990) Zircon U-Th-Pb and whole-rock Rb-Sr age patterns of lower Mesozoic igneous rocks in the Santa Rita Mountains, southeast Arizona: implications for Mesozoic magmatism and tectonics in the southern Cordillera. Geol Soc Am Bull 102:961–968. https://doi.org/10.1130/0016-7606(1990)102%3c0961:zu

Asmerom Y, Cheng H, Thomas RB, Hirschmann M, Edwards RL (2000) Melting of the Earth's lithospheric mantle inferred from protactinium–thorium–uranium isotopic data. Nature 406(6793):293–296. https://doi.org/10.1038/35018550

Bradtmiller LI, McManus JF, Robinson LF (2014) ^{231}Pa/^{230}Th evidence for a weakened but persistent Atlantic meridional overturning circulation during Heinrich Stadial 1. Nat Commun 5(1):5817. https://doi.org/10.1038/ncomms6817

Chase Z, Anderson RF, Fleisher MQ, Kubik PW (2003) Scavenging of ^{230}Th, ^{231}Pa and ^{10}Be in the Southern Ocean (SW Pacific sector): the importance of particle flux, particle composition and advection. Deep-Sea Res Part II Top Stud Oceanogr 50(3–4):739–768. https://doi.org/10.1016/s0967-0645(02)00593-3

Cheng H, Edwards RL, Hoff JA, Gallup CD, Richards DA, Asmerom Y (2000) The half-lives of uranium-234 and thorium-230. Chem Geol 169(1–2):17–33. https://doi.org/10.1016/S0009-2541(99)00157-6

Choi MS, Francois R, Sims K, Bacon MP, Brown-Leger S, Fleer AP, Ball L, Schneider D, Pichat S (2001) Rapid determination of ^{230}Th and ^{231}Pa in seawater by desolvated micro-nebulization Inductively coupled plasma magnetic sector mass spectrometry. Mar Chem 76(1–2):99–112. https://doi.org/10.1016/s0304-4203(01)00050-0

Deng F, Thomas AL, Rijkenberg MJA, Henderson GM (2014) Controls on seawater ^{231}Pa, ^{230}Th and ^{232}Th concentrations along the flow paths of deep waters in the Southwest Atlantic. Earth Planet Sci Lett 390:93–102. https://doi.org/10.1016/j.epsl.2013.12.038

Edmonds HN, Edwards RL, Moran SB, Hoff JA, Smith JN (1998) Protactinium-231 and thorium-230 abundances and high scavenging rates in the western Arctic Ocean. Science 280(5362):405–407. https://doi.org/10.1126/science.280.5362.405

Edwards RL, Cheng H, Murrell MT, Benjamin TM (1997) Protactinium dating of carbonates by thermal ionization mass spectrometry: implications for Quaternary climate change. Science 276(5313):782–786. https://doi.org/10.1126/science.276.5313.782

Edwards RL (1988) High precision thorium-230 age of corals and the timing of sea level fluctuations in the late Quaternary. Dissertation, California Institute of Technology, US

Hayes CT, Anderson RF, Fleisher MQ, Huang KF, Robinson LF, Lu Y et al (2014) ^{230}Th and ^{231}Pa on GEOTRACES GA03, the U.S. GEOTRACES North Atlantic transect, and implications for modern and paleoceanographic chemical fluxes. Deep-Sea Res Part II Top Stud Oceanogr 116:29–41. https://doi.org/10.1016/j.dsr2.2014.07.007

Hayes CT, Anderson RF, Fleisher MQ, Vivancos SM, Lam PJ, Ohnemus DC, Huang KF, Robinson LF, Lu YB, Cheng H, Edwards RL, Moran SB (2015) Intensity of Th and Pa scavenging partitioned by particle chemistry in the North Atlantic Ocean. Mar Chem 170:49–60. https://doi.org/10.1016/j.marchem.2015.01.006

Hoffmann SS, McManus JF, Curry WB, Brown-Leger LS (2013) Persistent export of ^{231}Pa from the deep central Arctic Ocean over the past 35,000 years. Nature 497(7451):603–606. https://doi.org/10.1038/nature12145

Jones RT, Merritt JS, Okazaki A (1986) A measurement of the thermal neutron capture cross section of ^{232}Th. Nucl Sci Eng 93:171–180. https://doi.org/10.13182/NSE86-A17666

Kretschmer S, Geibert W, Rutgers van der Loeff MM, Schnabel C, Xu S, Mollenhauer G (2011) Fractionation of ^{230}Th, ^{231}Pa, and ^{10}Be induced by particle size and composition within an opal-rich sediment of the Atlantic Southern Ocean. Geochim Cosmochim Acta 75(22):6971–6987. https://doi.org/10.1016/j.gca.2011.09.012

Lao Y, Anderson RF, Broecker WS, Hofmann HJ, Wolfli W (1993) Particulate fluxes of ^{230}Th, ^{231}Pa, and ^{10}Be in the northeastern Pacific Ocean. Geochim Cosmochim Acta 57(1):205–217. https://doi.org/10.1016/0016-7037(93)90479-g

Luo S, Ku TL (1999) Oceanic ^{231}Pa/^{230}Th ratio influenced by particle composition and remineralization. Earth Planet Sci Lett 167(3–4):183–195. https://doi.org/10.1016/s0012-821x(99)00035-7

Luo S, Ku TL (2004) On the importance of opal, carbonate, and lithogenic clays in scavenging and fractionating ^{230}Th, ^{231}Pa and ^{10}Be in the ocean. Earth Planet Sci Lett 220:201–211. https://doi.org/10.1016/s0012-821x(04)00027-5

Moran SB, Charette MA, Hoff JA, Edwards RL, Landing WM (1997) Distribution of ^{230}Th in the Labrador Sea and its relation to ventilation. Earth Planet Sci Lett 150(1–2):151–160. https://doi.org/10.1016/s0012-821x(97)00081-2

Moran SB, Shen CC, Weinstein SE, Hettinger LH, Hoff JA, Edmonds HN, Edwards RL (2001) Constraints on deep water age and particle flux in the Equatorial and South Atlantic Ocean based on seawater ^{231}Pa and ^{230}Th data. Geophys Res Lett 28(18):3437–3440. https://doi.org/10.1029/2001gl013339

Moran SB, Shen CC, Edmonds HN, Weinstein SE, Smith JN, Edwards RL (2002) Dissolved and particulate ^{231}Pa and ^{230}Th in the Atlantic Ocean: constraints on intermediate/deep water age, boundary scavenging, and ^{231}Pa/^{230}Th fractionation. Earth Planet Sci Lett 203(3–4):999–1014. https://doi.org/10.1016/s0012-821x(02)00928-7

Nozaki Y, Nakanishi T (1985) ^{231}Pa and ^{230}Th profiles in the open ocean water column. Deep-Sea Res 32(10):1209–1220. https://doi.org/10.1016/0198-0149(85)90004-4

Pickett DA, Murrell MT (1997) Observations of ^{231}Pa/^{235}U disequilibrium in volcanic rocks. Earth Planet Sci Lett 148(1–2):259–271. https://doi.org/10.1016/s0012-821x(97)00037-x

Pickett DA, Murrell MT, Williams RW (1994) Determination of femtogram quantities of protactinium in geologic samples by thermal ionization mass spectrometry. Anal Chem 66(7):1044–1049. https://doi.org/10.1021/ac00079a020

Robert J, Miranda CF, Muxart R (1969) Mesure de laperiode du protactionium 231 parmicrocalorimetrie. Radiochim Acta 11(2):104–108. https://doi.org/10.1524/ract.1969.11.2.104

Schlitzer R, Anderson RF, Dodas EM, Lohan M et al (2018) The GEOTRACES intermediate data product 2017. Chem Geol 493:210–223. https://doi.org/10.1016/j.chemgeo.2018.05.040

Shen CC, Cheng H, Edwards RL, Moran SB, Edmonds HN, Hoff JA, Thomas RB (2003) Measurement of attogram quantities of ^{231}Pa in dissolved and particulate fractions of seawater by isotope dilution thermal ionization mass spectroscopy. Anal Chem 75(5):1075–1079. https://doi.org/10.1021/ac026247r

Siddall M, Henderson GM, Edwards NR, Frank M, Müller SA, Stocker TF, Joos F (2005) ^{231}Pa/^{230}Th fractionation by ocean transport, biogenic particle flux and particle type. Earth Planet Sci Lett 237(1–2):135–155. https://doi.org/10.1016/j.epsl.2005.05.031

Thomas AL, Henderson GM, Robinson LF (2006) Interpretation of the ^{231}Pa/^{230}Th paleocirculation proxy: new water-column measurements from the southwest Indian Ocean. Earth Planet Sci Lett 241(3–4):493–504. https://doi.org/10.1016/j.epsl.2005.11.031

Thomas AL, Henderson GM, McCave IN (2007) Constant bottom water flow into the Indian Ocean for the past 140 ka indicated by sediment ^{231}Pa/^{230}Th ratios. Paleoceanography 22(4):PA4210. https://doi.org/10.1029/2007pa001415

Walter HJ, Rutgers van der Loeff MM, Hoeltzen H (1997) Enhanced scavenging of ^{231}Pa relative to ^{230}Th in the South Atlantic south of the Polar Front: implications for the use of the ^{231}Pa/^{230}Th ratio as a paleoproductivity proxy. Earth Planet Sci Lett 149(1–4):85–100. https://doi.org/10.1016/s0012-821x(97)00068-x

Walter HJ, Geibert W, Rutgers van der Loeff MM, Fischer G, Bathmann U (2001) Shallow vs. deep-water scavenging of and in radionuclide enriched waters of the Atlantic sector of the Southern Ocean. Deep-Sea Res 48(2):471–493. https://doi.org/10.1016/s0967-0637(00)00046-7

Publisher's Note